EBioMedicine 44 (2019) 502–515

Contents lists available at ScienceDirect

EBioMedicine

journal homepage: www.ebiomedicine.com

EBioMedicine
Published by THE LANCET

Research paper

# Treatment of keratinocytes with 4-phenylbutyrate in epidermolysis bullosa: Lessons for therapies in keratin disorders

Marina Spörrer [a], Ania Prochnicki [b], Regine C. Tölle [c], Alexander Nyström [d], Philipp R. Esser [d], Melanie Homberg [e], Ioannis Athanasiou [d], Eleni Zingkou [d], Achim Schilling [a,f], Richard Gerum [a], Ingo Thievessen [a], Lilli Winter [b], Leena Bruckner-Tuderman [d], Ben Fabry [a], Thomas M. Magin [e], Jörn Dengjel [c,d], Rolf Schröder [b], Dimitra Kiritsi [d,*]

[a] Department of Physics, Friedrich-Alexander-University Erlangen-Nuremberg, Erlangen, Germany
[b] Institute of Neuropathology, Friedrich-Alexander-University Erlangen-Nuremberg, Erlangen, Germany
[c] Department of Biology, University of Fribourg, Switzerland
[d] Department of Dermatology, Medical Center - University of Freiburg, Faculty of Medicine, University of Freiburg, Freiburg, Germany
[e] Institute of Biology and SIKT, University of Leipzig, Leipzig, Germany
[f] Experimental Otolaryngology, ENT Hospital, Head and Neck Surgery, Friedrich-Alexander University Erlangen-Nuremberg, Erlangen, Germany

ARTICLE INFO

*Article history:*
Received 19 November 2018
Received in revised form 30 April 2019
Accepted 30 April 2019
Available online 9 May 2019

*Keywords:*
Keratins
Skin blistering
Keratinocyte
Epidermolysis bullosa
4-PBA

ABSTRACT

*Background*: Missense mutations in keratin 5 and 14 genes cause the severe skin fragility disorder epidermolysis bullosa simplex (EBS) by collapsing of the keratin cytoskeleton into cytoplasmic protein aggregates. Despite intense efforts, no molecular therapies are available, mostly due to the complex phenotype of EBS, comprising cell fragility, diminished adhesion, skin inflammation and itch.
*Methods*: We extensively characterized *KRT5* and *KRT14* mutant keratinocytes from patients with severe generalized EBS following exposure to the chemical chaperone 4-phenylbutyrate (4-PBA).
*Findings*: 4-PBA diminished keratin aggregates within EBS cells and ameliorated their inflammatory phenotype. Chemoproteomics of 4-PBA-treated and untreated EBS cells revealed reduced IL1β expression- but also showed activation of Wnt/β-catenin and NF-kB pathways. The abundance of extracellular matrix and cytoskeletal proteins was significantly altered, coinciding with diminished keratinocyte adhesion and migration in a 4-PBA dose-dependent manner.
*Interpretation*: Together, our study reveals a complex interplay of benefits and disadvantages that challenge the use of 4-PBA in skin fragility disorders.


## 1. Introduction

Epidermolysis bullosa simplex (EBS) is characterized by skin fragility manifesting with blisters and erosions caused by minor mechanical trauma. At the ultrastructural level, EBS is characterized by intraepidermal tissue separation. The phenotype ranges from relatively mild blistering of the hands and feet to severe generalized blistering. The repeated palmoplantar blistering leads to progressive hyperkeratosis of the palms and soles, which begins in childhood and is the major concern for affected adult individuals. Mucosal involvement in severe generalized EBS (EBS sev gen) may interfere with feeding, especially in neonates and infants [1]. The disease is primarily caused by dominantly inherited mutations in the keratin 5 (*KRT5*) or 14 genes (*KRT14*). KRT5 and KRT14 form extremely stable dimer and tetramer subunits. The resulting intermediate filaments organize themselves into cross-linked networks. Their structural support function is lost, if one of the proteins is disturbed due to mutations [2].

In the past, heat stress-induced keratin aggregation has been observed in primary keratinocytes derived from EBS patients [3]. However, primary keratinocytes possess a limited lifespan and heterogeneous behavior with increasing passage numbers, making them unsuitable for more extensive functional assays. A large part of the pathophysiological work on EBS is based on animal models, which cannot

*Abbreviations:* EBS, epidermolysis bullosa simplex; EDTA, ethylenediaminetetraacetic acid; HS, heat shock; IF, intermediate filaments; IIF, Indirect immunofluorescence staining; KRT5mut, *KRT5*-mutated cells; KRT5mut+, *KRT5*-mutated, 4-PBA-treated cells; KRT14mut, *KRT14*-mutated cells; KRT14mut+, *KRT14*-mutated, 4-PBA-treated cells; NHK, normal human keratinocytes; NHK+, normal human keratinocytes, treated with 4-PBA; OA, ocadaic acid; 4-PBA, 4-phenylbutyrate.

* Corresponding author at: Department of Dermatology, Medical Faculty, Medical Center- University of Freiburg, Hauptstrasse 7, 79104 Freiburg, Germany.
*E-mail address:* dimitra.kiritsi@uniklinik-freiburg.de (D. Kiritsi).

https://doi.org/10.1016/j.ebiom.2019.04.062

**Research in context**

*Evidence before this study*

4-PBA has been suggested to work as an anti-aggregation agent in genetic skin fragility disorders. Therefore, a therapeutic potential has been assumed and indeed preliminary in vitro data have suggested disease ameliorating benefit of 4-PBA on the cellular level.

*Added value of this study*

Here we conducted a detailed analysis of the therapeutic applicability of 4-PBA not only assessing its anti-aggregating modalities in the setting of epidermolysis bullosa simplex due to impaired functionality of keratin filaments, but also its larger contextual actions and outcomes. 4-PBA was tested over a range of concentrations in multiple donor-derived materials and with different analytical techniques, ranging from targeted to global analyses.

*Implications of all the available evidence*

Our study indicates low dose 4-PBA has some favorable effects on epidermolysis bullosa simplex keratinocytes, although it comes with some potentially unfavorable side effects. Collectively, weighing the advantages and disadvantages of 4-PBA in the setting of epidermolysis bullosa simplex reveals that it cannot be considered a good therapeutic candidate. However, other less broad spectrum molecular chaperones targeting aggregate formation and ER stress could represent possible therapeutic tools. Their effects on cellular adhesion and migration must first be carefully investigated.

accurately recapitulate the disease, since mouse skin is anatomically different from human skin [4]. In addition, there are significant differences between different mouse models and affected mice die soon after birth [5–7]. We and others [8–12] have established patient-derived immortalized cell lines as a reproducible EBS model to characterize the role of intermediate filament (IF) protein aggregates in EBS keratinocytes and the cellular response of EBS keratinocytes to thermal and chemical stress. As published reports imply differences between *KRT5* and *KRT14*-mutated cells [13], in the present study we investigated cells from patients with common missense *KRT5* and *KRT14* mutations to better understand the molecular consequences and underlying disease mechanisms.

4-phenylbutyrate (4-PBA) is an approved orphan drug, which is used to treat urea cycle disorders, as its metabolites offer an alternative pathway to allow for the excretion of excess nitrogen. 4-PBA has been shown to facilitate protein folding, suppressing ER stress-mediated apoptosis by inhibiting eukaryotic initiation factor 2a (eIF2a) phosphorylation, CCAAT (highly conserved promoter region of the Grp genes)/enhancer-binding protein homologous protein (CHOP) induction, and caspase-12 activation [14,15]. The chemical chaperone 4-PBA has also been shown to antagonize protein aggregation in several genetic and inflammatory disorders, e.g. muscular dystrophies/ myopathies [16,17] and Parkinson's disease [18]. Currently, 49 clinical trials are listed in the ClinicalTrials.gov registry. Notably, small pilot studies have been performed with keratinocytes of skin fragility patients. 4-PBA reduced the formation of specifically heat-induced keratin aggregates in EBS cells [3] and increased mRNA and protein levels of the mutant protein kindlin-1 in cells of a Kindler syndrome patient [19]. It also improved cell spreading and proliferation in a recombinant system [19]. In cells of patients with epidermolytic ichthyosis due to *KRT1* or *KRT10* mutations, 4-PBA treatment reduced the fraction of aggregate-containing cells, but also impaired mRNA expression of keratins 1 and 10 [20]. 4-PBA was determined to be effective in patients with progressive familial intrahepatic cholestasis [21], and trials are ongoing for spinal muscular atrophy and thalassemia.

In the present study, we took an interdisciplinary approach using molecular, cell-biochemical and proteomics methods, to characterize the effects of 4-PBA on keratinocytes derived from patients with EBS. 4-PBA treatment diminished the presence of keratin aggregates within EBS cells and ameliorated their inflammatory phenotype; however, it negatively impacted keratinocyte adhesion and migration in a dose-dependent manner. Together, our study reveals a complex interplay of benefits and disadvantages that challenge the use of 4-PBA in skin fragility disorders.

## 2. Results

### 2.1. 4-PBA reduces keratin aggregation in EBS keratinocyte lines

We generated HPV16-E6E7 immortalized control keratinocytes from three healthy human subjects and from five patients with severe generalized EBS. Two patients were heterozygous carriers of the common *KRT5* mutation p.E477K, and three were heterozygous carriers of the most common *KRT14* mutation p.R125C. The patients had different ages (9 days to 52 years old), but all suffered from widespread blistering with early development of palmoplantar keratoderma (Supplemental Fig. 1).

A first observation revealed that only EBS keratinocyte and not control cell lines, display low degrees of IF aggregates, visualized as keratin clumping, even at resting state. Around 4% of *KRT5*-mutated (KRT5mut) and 30% of *KRT14*-mutated (KRT14mut) cells contained aggregates, as shown by the staining with a keratin 5 antibody (Fig. 1A and B upper panel). To analyze whether the chemical chaperone 4-PBA has the capacity to reduce those aggregates, cells were treated for 24 h with 1 mM 4-PBA or left untreated. 4-PBA treatment resulted in a significant reduction in the fraction of cells with keratin aggregates in both KRT5mut and KRT14mut keratinocytes (Fig. 1B, lower panel). To analyze whether 4-PBA exhibits a time- dependent mode of action, the cell lines were also treated for 48 h with 1 mM 4-PBA. This, however, did not result in a significant further reduction compared to 24 h treatment (Fig. 1B, lower panel).

### 2.2. 4-PBA reduces the vulnerability of keratin IF networks to thermal and chemical stress

To investigate how 4-PBA affects the response of EBS keratinocyte cell lines to chemical stress, we treated the cells for 2 h with 0.1 μg/ml ocadaic acid (OA), a serine/threonine phosphatase inhibitor that induces a dynamic disassembly of the keratin IF networks due to their hyper-phosphorylation [22].

In analogy to experiments with murine plectin-deficient keratinocytes [23], the course of the dynamic disassembly of the keratin IF networks was also detected in our human keratinocyte cell lines. Upon OA treatment, the formerly well-spread keratin IF network of the EBS keratinocyte cell lines formed thick bundles of filaments, that collapsed towards the nucleus (Fig. 1C, yellow arrows). The impact of OA treatment in EBS keratinocytes was considerably more pronounced than in control cells: around 40% of the KRT5mut cells and 80% of KRT14mut cells displayed different degrees of aggregate formation. Critically, the addition of 1 mM 4-PBA for 24 h before the OA treatment had a moderate stabilizing effect on the IF network, which was significant both in the *KRT14*- and *KRT5*-mutated keratinocytes (Fig. 1C).

Next, we analyzed the effects of thermal stress on the IF network of keratinocytes. Cells were either subjected to a heat shock treatment for 30 min at 43 °C or left untreated. Cells were then stained with a keratin 5 antibody to detect keratin aggregates. After heat shock, both the KRT5mut and KRT14mut cell lines showed significant increase in the percentage of cells with perinuclear keratin aggregates. Comparable to their response to chemical stress, the KRT14mut keratinocytes (60% of cells with keratin aggregates) were also more susceptible to thermal

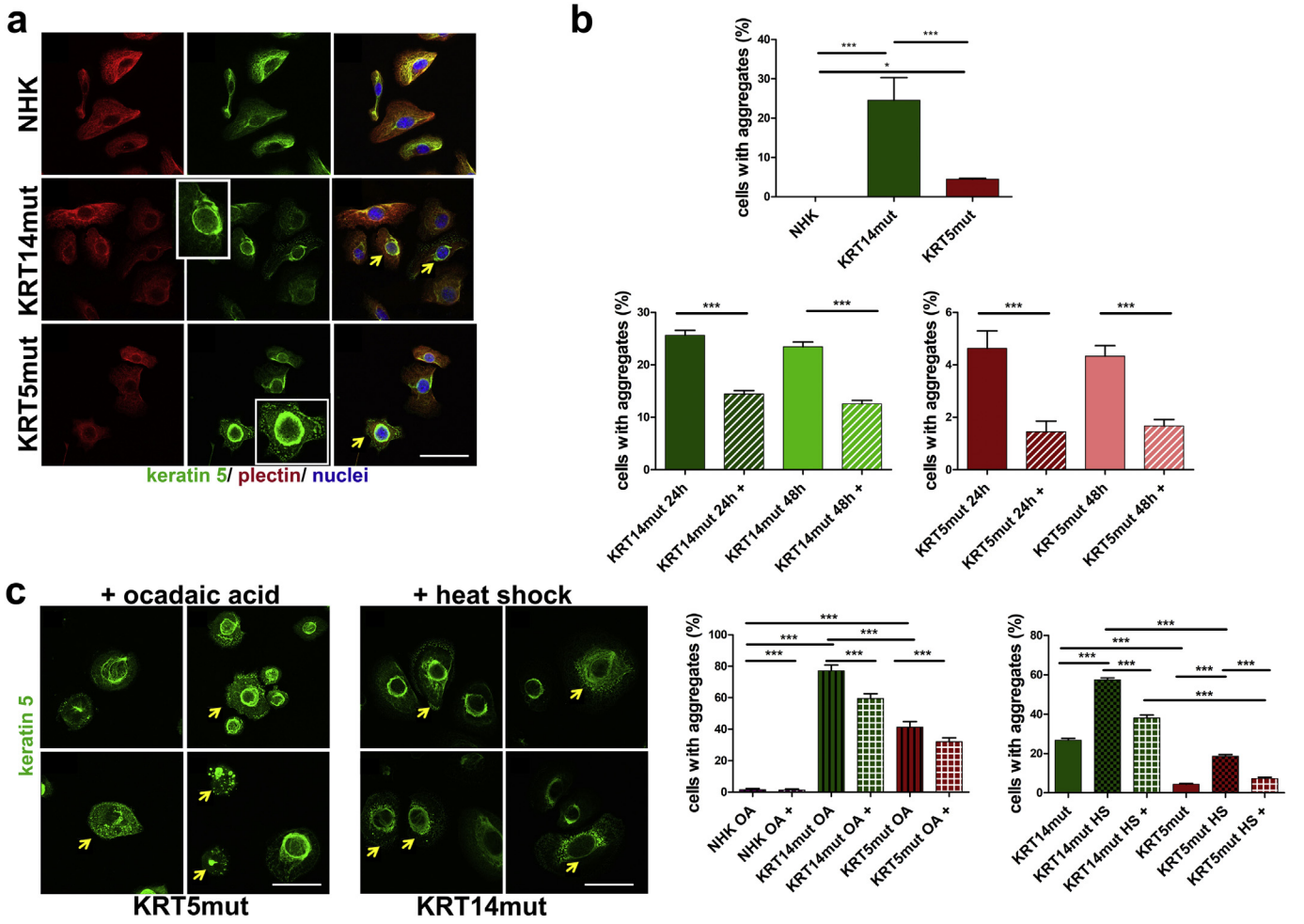


**Fig. 1.** Keratin aggregates in EBS keratinocytes at resting state and after stress: rescue by 4-PBA. A Analysis of the subcellular localisation of plectin and keratin 5 as shown by immunofluorescence staining of control normal human keratinocytes (NHK), keratinocytes from patients with mutations in the keratin 14 gene (KRT14mut) and keratinocytes from patients with mutations in the keratin 5 gene (KRT5mut) with anti-plectin [Alexa555 (Cy3; red)] and keratin 5 [Alexa488 (GFP; green)] antibodies. Yellow arrows depict cells with aggregates of their keratin IF network. Scale bar: 50 μm. B The upper panel shows quantification of the keratinocytes with aggregates. The NHKs show no aggregates at resting state, whereas they are significantly more in KRT14mut than KRT5mut cells (for NHK versus KRT14mut ***P: 0.0001, for NHK versus KRT5mut *P: 0.0211 and for KRT5mut versus KRT14mut ***P: 0.0004, all done with student's *t*-test). In the lower panel the percentage of cells before (NHK, KRT14mut, KRT5mut) and after use of 4-PBA (NHK+, KRT14mut+, KRT5mut+) is shown. The data are presented as mean ± SEM. Intermediate filament (IF) aggregates are significantly less in cells treated with 1 mM 4-PBA [KRT14mut (***$P < .0001$, student's *t*-test) and KRT5mut + cells (***P < .0001, student's t-test)], irrespective of the treatment time (24 or 48 h). C Immunofluorescence staining for keratin 5 of EBS cells upon ocadaic treatment (OA) and upon heat-shock (HS). In the 4 subimages, different KRT5mut and KRT14mut cells are shown, highlighting the different appearances of the cells. The well-spread keratin IF network, as seen in NHK in A, forms thick bundles of filaments in several EBS keratinocytes, which seem to collapse towards the nucleus (yellow arrows). On the left quantification graph, the percentage of keratinocytes with aggregates before (NHK OA, KRT14mut OA, KRT5mut OA) and after use of 4-PBA (NHK OA+, KRT14mut OA+, KRT5mut OA+) are shown. The experiments were done in triplicates; the average of the three experiments is shown. The use of 4-PBA significantly reduces the number of cells with aggregates after OA treatment [NHK-treated cells (NHK OA+), KRT14mutated-treated cells (KRT14mut +) and KRT5mutated-treated cells (KRT5mut+): for all ***P < .0001, student's *t*-test]. EBS keratinocytes treated with HS (KRT14mut HS and KRT5mut HS) showed significant induction of aggregate formation [for both KRT14mut vs KRT14mut HS and KRT5mut vs KRT5mut HS ***P < .0001, student's t-test], which was reversed after 4-PBA use [KRT14mut HS+ and KRT5mut HS+ ***P < .0001, student's t-test]. Scale bar: 50 μm.

stress than the KRT5mut cells (20% of cells with keratin aggregates). 4-PBA treatment significantly reduced keratin aggregation after heat shock (Fig. 1C).

Our data suggest that the presence of IF aggregates in EBS keratinocytes is mutation-dependent and more pronounced in KRT14mut cells. In combination with chemical or thermal stress, mutations in both genes trigger extensive keratin aggregation, that could be partially prevented by treatment of the keratinocytes with 1 mM 4-PBA for 24 h, whereas longer treatment did not further enhance the positive effects.

### *2.3. 4-PBA negatively impacts cell adhesion, migration and formation of cell-cell contacts*

EBS is a skin fragility disorder accompanied by weakened epithelial sheet integrity. Thus, we next assessed the effects of the 4-PBA treatment on keratinocyte adhesion with use of two different assays, to evaluate cell-cell and cell-extracellular matrix (ECM) adhesion. In the dispase-based dissociation assay, cells were treated with dispase for 30 min and then subjected to inversion. EBS keratinocytes dissociated easier than the control cells (Fig. 2A). We next investigated the effect of 4-PBA treatment on keratinocyte adhesion structures. After 1 mM 4-PBA administration, we observed diminished cell-cell contacts, as visualized by desmoplakin, plakoglobin (Fig. 2B) and E-cadherin staining (Fig. 6A). Although this was not always statistically significant, we also observed reduced total amounts of these proteins as revealed by immunoblotting (Fig. 2C, significance shown in the figure legend). Besides lower abundance, both plakoglobin and desmoplakin did not localize to cell-cell junctions, as is seen in untreated cells (Fig. 2B, white arrows). Upon 4-PBA treatment no significant differences in the abundance of KRT14 and its binding partners KRT17 and KRT16 were observed. KRT6 was enhanced after 4-PBA treatment, possibly as a

compensatory mechanism to the reduced adhesion [24] or alternatively due to increased proliferation (Supplemental Figs 2 and Fig. 6B).

Cell-ECM adhesion was evaluated with two different assays. First, we evaluated the effect of 4-PBA treatment on keratinocyte adhesion on uncoated tissue culture plastic. This adhesion was normalized to adhesion on collagen I (Col1) coating, representing F-actin and keratin based ECM adhesion [25], for each cell type. The EBS keratinocytes adhered with higher force than the control cells (Fig. 3A), this effect was statistically significant only for the KRT14mut cells. After adding 4-PBA, adhesiveness was unaltered in control cells, but decreased in EBS keratinocytes (Fig. 3A). Second, using the spinning disk assay [26], we estimate the adhesiveness of cells to the ECM by applying different fluid shear stresses to adherent cells, and measuring the fraction of cells that remain attached in this process. This assay is relevant for the in vivo situation of keratinocytes, where they are exposed to high mechanical stresses. The fraction of adherent cells was higher in EBS keratinocytes compared to control cells (Fig. 3B, left panel). 4-PBA treatment resulted in significantly lower numbers of adherent cells, both NHK and EBS (Fig. 3B, right panel). Thus, all three assays show that 4-PBA impaired both cell-cell and cell-ECM adhesion in control, and even more so in KRT5mut and KRT14mut cells. Impairment of cell-cell adhesion due to 4-PBA treatment was dose-dependent. After treatment with 1 mM 4-PBA the cells detached at a ~twofold higher rate in the dispase-dissociation assay (Fig. 2A), whereas after treatment with 10 mM 4-PBA they detached at a ~tenfold higher rate (Supplemental Fig. 3A, left panel). Similar effects were observed with the keratinocyte adhesion to the underlying uncoated tissue culture plastic (Supplemental Fig. 3A, right panel).

We then analyzed the effect of 4-PBA on cell migration with an in vitro wound healing assay. EBS keratinocytes migrated faster than control cells; this was especially pronounced in the KRT5mut cells, where the wound area was completely closed within 9 h (Supplemental Fig. 4A and B). Treatment with 4-PBA considerably inhibited cellular migration. In the control keratinocytes around 70% of the wound area was closed after 9 h, whereas after 1 mM 4-PBA treatment only 60% of the wound area was closed. The KRT5mut cells closed the wound area within 9 h, whereas around 10% of the area remained open when the cells were treated with 1 mM 4-PBA. For the KRT14mut cells, the effects were even more pronounced. Untreated KRT14mut cells almost closed the wound area within 9 h, whereas with 1 mM 4-PBA treatment >45% of the wound area was still open (Supplemental Fig. 4C). The impact of 4-PBA treatment on cell migration was dose-dependent; cell migration nearly stopped at a dose of 10 mM 4-PBA (Supplemental Fig. 3). To understand the deleterious effects of 4-PBA on EBS cell migration, we also stained for the focal adhesion-associated molecules integrin β1 and for F-actin, as visualized by phalloidin. Integrin β1 was greatly enhanced after 4-PBA treatment especially in control and KRT5mut cells, probably as a compensatory mechanism to long-term reduced adhesion (Fig. 3C). 4-PBA treatment resulted in altered staining of the epidermal F-actin cytoskeleton in control and EBS keratinocytes, whereas the total amount of F-actin was unchanged, as shown by immunoblotting, suggesting altered distribution of the actin filaments in the cells (Fig. 3D). Although values did not reach statistical significance, we also found increased abundance of laminin-332 in cells after 4-PBA treatment (Fig. 3E). This correlated with the reduced motility of the treated keratinocytes [27] (Supplemental Fig. 3). Together, our data highlight that 4-PBA treatment impairs adhesion and migration of EBS keratinocytes, despite upregulation and re-organization of several proteins involved in adhesion and migration. These effects are dose-dependent; higher 4-PBA concentrations inhibit keratinocyte migration (Supplemental Fig. 3B) and cause detachment of the cells.

### 2.4. 4-PBA reduces apoptosis and inflammatory signaling in EBS cells

To assess the effects of long-term 4-PBA treatment on cell fitness, we treated primary control human keratinocytes (NHK) with 1 mM and 5 mM 4-PBA every 2 days for 1 week or left the cells untreated. Keratinocytes growth was evaluated with the colony-forming efficiency assay, which showed that 4-PBA treatment reduced cell growth, as quantified by the colony size (Fig. 4A). In addition, the colony size decreased with increasing 4-PBA dosage, indicating that 4-PBA treatment either reduces keratinocytes proliferation or enhances cell death, e.g. by apoptosis. Enhanced apoptosis has been described as a possible pathogenetic mechanism in genetic disorders with aggregate formation [28]. Thus, we visualized apoptotic cells by flow cytometry using the Annexin V binding assay. We found increased numbers of apoptotic cells (statistically significant for EBS cells in late apoptosis) in EBS keratinocyte cell lines compared to the control keratinocytes, irrespective of the underlying keratin mutations. EBS cells have been reported to be more susceptible to apoptosis [29,30], although in at least one report, *KRT14* mutant cells showed higher resistance to apoptosis following mechanical stress- that was reversed by inhibiting ERK [10]. 4-PBA treatment had divergent effects in NHK and EBS cells. In NHK cells, it induced apoptosis. In EBS cells, apoptosis decreased after 4-PBA, possibly as a result of the reduced aggregates (Fig. 4B). Apoptosis has also been linked to inflammation and to increased IL1β levels [31]. IL1β is a potent player in cutaneous inflammation and has been proposed to be highly expressed in EBS skin [32]. Thus, we evaluated the expression of IL1β in untreated and 4-PBA-treated NHK and EBS cells. We found significantly enhanced IL1β levels in EBS cells, whereas 4-PBA treatment reduced IL1β levels (Fig. 4C), thus linking enhanced IL1β to the presence of pathogenic keratin IF aggregates in EBS pathogenesis. Intriguingly, treatment of NHK cells with 1 mM 4-PBA resulted in enhanced IL1β levels (Fig. 4C).

### 2.5. Global proteomics analysis reveals reduced expression of desmosomal and ECM molecules

To gain a better understanding on how 4-PBA treatment influenced molecular processes in EBS, we performed unbiased mass spectrometry-based proteomics of control and EBS keratinocyte cell lines. Two different cell lines for each group, control (NHK), KRT5mut and KRT14mut cells, were metabolically labeled using stable isotope labeling by amino acids in cell culture (SILAC) [33]. Differentially labeled cells, untreated and treated with 4-PBA respectively, were mixed, lysed in SDS buffer, proteins were separated by SDS–PAGE and digested in-gel using trypsin. The resulting peptide mixtures were analyzed by quantitative liquid chromatography-mass spectrometry. In total 3′292 proteins were identified, of which 2′779 could be quantified in at least one sample. Of these, 1′097 were present in all samples and employed for further analysis using hierarchical clustering (Supplemental Table 1). Changes in the proteomic composition after 4-PBA treatment are presented as a heat map (Fig. 5A) and show that KRT5mut and KRT14mut cells clustered together, highlighting global, EBS-specific differences after 1 mM 4-PBA treatment compared to NHK cells (Fig. 5A). Two large clusters were identified comprising differentially, co-regulated proteins in EBS, clusters 7 and 12 (Fig. 5A). GO term analysis of respective proteins revealed enrichment of the GO terms “cellular or carboxylic acid metabolic process” and “catabolic process” in cluster 12, whereas in cluster 7 terms related to “cell adhesion”, “actin cytoskeleton and extracellular matrix organization” and “developmental process” were enriched (Fig. 5A). This indicates that 4-PBA impacts cell adhesion and organization of both the actin cytoskeleton and the ECM more strongly in EBS cells than NHK cells. In addition, to uncover cellular pathways responsive to 4-PBA treatment that are common in NHK and EBS cells, we compared treated versus non-treated cells and analyzed significantly regulated proteins on potential interactions. We constructed two networks of significantly regulated proteins after 4-PBA treatment in NHK and EBS cells (Fig. 5B). These included mostly proteins of the cytoskeleton and the extracellular matrix. Also, proteins involved in ubiquitination were detected.

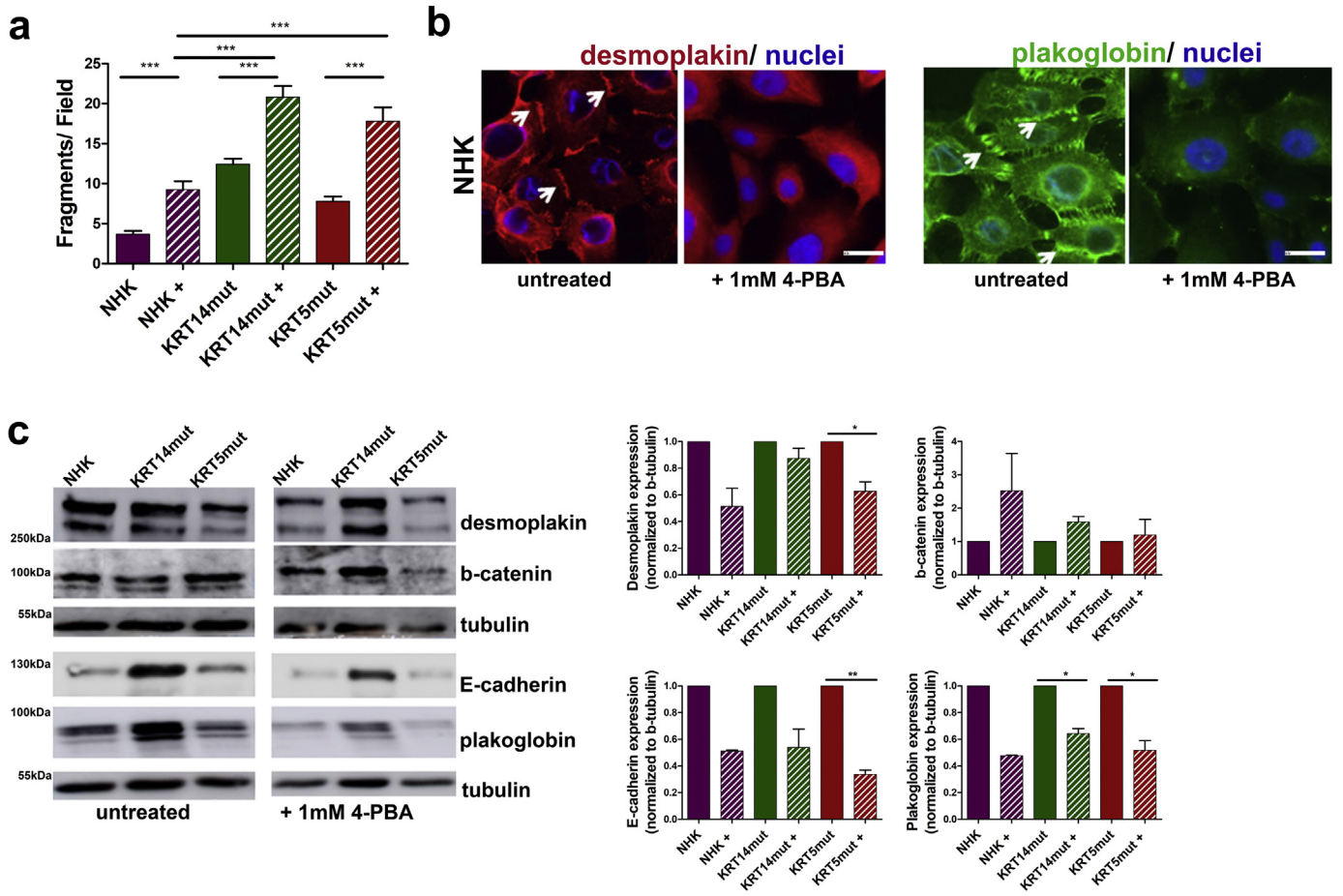


**Fig. 2.** 1 mM 4-PBA results in loss of cell-cell adhesion through diminished cell-cell contacts. A In the dispase-based dissociation assay the 1 mM 4-PBA-treated cells detached significantly easier resulting in more fragments and thus reflecting disturbed cell-cell contacts [for NHK+, KRT14mut + and KRT5mut+: ***P < .0001, student's t-test]. B Immunofluorescence staining with anti-desmoplakin (red) antibodies to visualize desmosomes, and anti-plakoglobin (green) antibodies to demonstrate adherence junctions, in NHK was performed after calcium switch. Both were reduced and their localization at the cell-cell junctions was lost after treatment with 1 mM 4-PBA. Scale bar: 50 μm. C Immunoblotting for desmoplakin, E-cadherin and plakoglobin revealed reduced abundance after 1 mM 4-PBA treatment, whereas β-catenin was found enhanced. Bar graphs on the right show expression of these proteins normalized to tubulin as percentage of expression in untreated cells [desmoplakin: $P = .2383$ for KRT14mut and $^{*}P = .0343$ for KRT5mut; E-cadherin: $P = .0787$ for KRT14mut and $^{**}P = .0023$ for KRT5mut; β-catenin: $P = .0675$ for KRT14mut and $P = .7116$ for KRT5mut; plakoglobin: $^{*}P = .110$ for KRT14mut and $^{*}P = .0220$ for KRT5mut, all done with paired student's *t*-test].

Mass spectrometry revealed that the abundance of several additional cytoskeletal proteins, among them desmoplakin and other members of the plakin family, was reduced after 4-PBA treatment (Fig. 5B). In addition, several ECM proteins were reduced both in NHK and EBS cells, e.g. thrombospondin 1, fibronectin and collagen VII, as confirmed by immunoblotting (Fig. 5C). After 4-PBA treatment of NHK, the expression of all proteins was reduced but reached statistical significance only for collagen VII. Physiologically, these proteins are associated with wound healing response, explaining the adverse effects of 4-PBA on cell-matrix adhesion and defective wound closure.

### *2.6. Proteomics reveals co-induction of the NF-kB and Wnt signaling pathways*

Furthermore, proteomics revealed additional significantly deregulated proteins that are linked to enhanced cell proliferation and activation of the NF-κB pathway. Selected molecules were further analyzed for their expression on mRNA level with qPCR. PPFIA4, a member of the liprin family associated with epithelial contact formation, was enhanced in the proteome and the quantitative PCR (qPCR) after 4-PBA, probably as a compensatory approach to cellular dissociation [34] (Supplemental Fig. 5). The PPFIA4 gene promoter is activated after binding of the hypoxia-inducible factor 1α, a molecule linked to NF-κB signaling. Similarly, the HECT-domain ubiquitin ligase HERC3 [35], amphiregulin [36] and the low-density lipoprotein receptor-related protein 1 (LRP1) [37] were significantly ($P < .05$) upregulated after 1 mM 4-PBA treatment at the protein level. Measurements at the mRNA level confirm this observation, although not all data points reached statistical significance.

The 4-PBA-induced abundance of molecules involved in NF-κB activation in keratinocytes, prompted a more detailed investigation of this pathway. E-cadherin was reduced by 4-PBA, but we also noted some round vesicles around the nucleus (Fig. 6A), an indication of perinuclear accumulation of E-cadherin, which is known to activate both the NF-κB and Wnt/ β-signaling pathways [38]. Both pathways are implicated in cell proliferation, which increased dose-dependently in 4-PBA-treated cells (Fig. 6B and Supplemental Fig. 3C). The NF-κB pathway is a central regulator of inflammation and modulates a spectrum of biological processes; it can be activated by canonical and non-canonical pathways [39]. In the canonical pathway, (RelA/p65)/p50 heterodimers are maintained in the cytoplasm in an inactive state by a family of inhibitors of NF-κB (IKBα). These IKBα inhibitors were expressed at lower levels in EBS cells compared to NHK before treatment, although there was some variation between the KRT14mut cell lines. After 4-PBA treatment, the expression of IKBα inhibitors decreased even more (Fig. 6C). Upon activation of the pathway, IKBα becomes phosphorylated leading to its degradation and the subsequent release of the RelA/p50 heterodimer. These newly liberated RelA/p50 heterodimers can translocate to

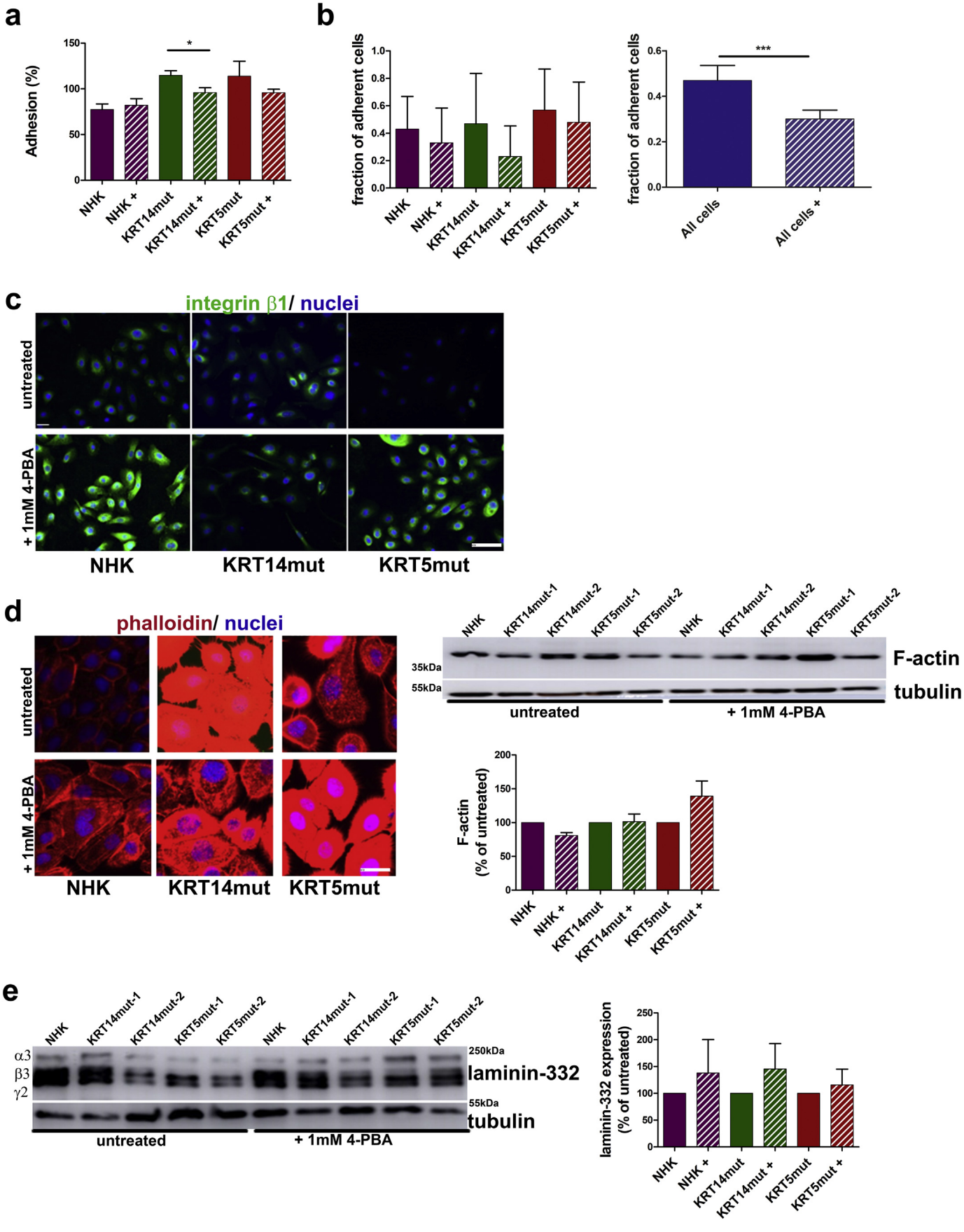
a
Adhesion (%)
150
100
50
0
*
NHK
NHK +
KRT14mut
KRT14mut +
KRT5mut
KRT5mut +
b
fraction of adherent cells
1.0
0.8
0.6
0.4
0.2
0.0
NHK
NHK +
KRT14mut
KRT14mut +
KRT5mut
KRT5mut +
fraction of adherent cells
0.6
0.4
0.2
0.0
***
All cells
All cells +
c
integrin β1/ nuclei
untreated
+ 1mM 4-PBA
NHK
KRT14mut
KRT5mut
d
phalloidin/ nuclei
untreated
+ 1mM 4-PBA
NHK
KRT14mut
KRT5mut
NHK
KRT14mut-1
KRT14mut-2
KRT5mut-1
KRT5mut-2
NHK
KRT14mut-1
KRT14mut-2
KRT5mut-1
KRT5mut-2
35kDa
55kDa
F-actin
tubulin
untreated
+ 1mM 4-PBA
F-actin (% of untreated)
200
150
100
50
0
NHK
NHK +
KRT14mut
KRT14mut +
KRT5mut
KRT5mut +
e
NHK
KRT14mut-1
KRT14mut-2
KRT5mut-1
KRT5mut-2
NHK
KRT14mut-1
KRT14mut-2
KRT5mut-1
KRT5mut-2
α3
β3
γ2
250kDa
laminin-332
55kDa
tubulin
untreated
+ 1mM 4-PBA
laminin-332 expression (% of untreated)
250
200
150
100
50
0
NHK
NHK +
KRT14mut
KRT14mut +
KRT5mut
KRT5mut +

the nucleus to activate the transcription of a diverse range of inflammatory mediators, such as COX2, TNFα, and IL-6 [39]. Indeed, after 4-PBA treatment in both NHK and EBS cell lines IKBα and ERK were more phosphorylated (Fig. 6C), which is also in line with the observed increased proliferation (Fig. 6B and Supplemental Fig. 3C).

Intriguingly, TNFα was upregulated after 4-PBA treatment (Supplemental Fig. 6), probably as a result of negative regulation of IL1β [40] (Fig. 6C). The NF-κB pathway either positively or negatively regulates Wnt / β-catenin signaling, which exerts both anti-inflammatory and proinflammatory functions [41]. β-Catenin is a central mediator of the Wnt signaling cascade and functions as an adhesion molecule, linking E-cadherin to the actin cytoskeleton. In the absence of Wnt stimulation, β-catenin in the cytoplasm is constitutively targeted for degradation. Upon Wnt activation, the degradation complex is inactivated, resulting in cytoplasmic accumulation of β-catenin. After translocation into the nucleus, β-catenin associates with T cell factor/lymphoid enhancer factor (TCF/LEF1) transcription factor and promotes the transcription of its target genes. Here, we observed enhanced LEF1 staining after 4-PBA treatment in the EBS cells, whereas β-catenin was the only adhesion molecule that was found upregulated after 4-PBA in immunoblot (Fig. 2C), having lost its localization at the cell-cell contacts (Fig. 6D and Supplemental Fig. 7A). These results indicate that the Wnt signaling pathway is also activated upon 4-PBA treatment.

### 2.7. 3D skin equivalents confirm results on cellular level

To test whether the beneficial or adverse effects of 4-PBA on EBS-cells are critical in a more physiological, tissue-like environment and since no viable EBS animal model is available, we used three-dimensional (3D) skin equivalents. The skin equivalents were developed by use of control keratinocytes vs EBS cells for the epidermal part, and normal human fibroblasts for the dermal part. The skin equivalents grew in their chambers for 4 weeks, in which they were treated 3 x weekly with 1 mM 4-PBA. We observed a few areas of dermo-epidermal detachment in the EBS skin equivalents, but not in the controls. In the 4-PBA treated equivalents, however, several intra- and subepidermal splits were found (Fig. 7A, black arrows; 7B and C, yellow arrows). Laminin-332 and integrin β4 showed abnormal staining patterns after 4-PBA treatment in the NHK and EBS skin equivalents (Fig. 7 B and C). Laminin-332 deposition was irregular and patchy in the NHK, whereas it also stained the suprabasal keratinocytes in the EBS cells. Similarly, integrin β4 had a more pronounced, irregular, suprabasal patchy expression in the treated skin equivalents. Thus, 4-PBA treatment perturbs laminin-332 organization, which in turn seems to abrogate the polarized expression of integrin α6β4 in basal keratinocytes. β-catenin showed a more cytoplasmic localization in the EBS skin equivalents, having lost its localization at the cell-cell contacts, which was even more pronounced in the treated EBS, but also the treated NHK skin equivalents (Supplemental Fig. 7A). Finally, nuclear localization of the p65 subunit of NF-κB was significantly increased in the epidermal part of the treated NHK and EBS skin equivalents, indicative of activation of the transcription factor (Supplemental Fig. 7B). This 3D model, as a straight-forward approach to imitate the situation in the human skin, confirmed our previous results on cellular level. Together, our data highlight that 4-PBA has a dose-dependent negative impact on cell adhesion and migration in the skin.

## 3. Discussion

EBS is an inherited skin fragility disorder with so far only symptomatic treatment options so far. In the last years therapies aiming at symptom-relief have gained attention in the field of genetic disorders. Although some successful curative therapy approaches have been described for other types of EB [42], their clinical implementation still lies in distant future. Symptom-relief therapies are being developed on the basis of detailed knowledge of molecular and cellular pathogenetic mechanisms; they target key molecules involved in major symptoms. In case of EBS, the *KRT5* and *KRT14* mutations induce IF network aggregates within the keratinocytes and cause reduced resilience to mechanical stress. The presence of the aggregates is mutation-dependent, but also dependent on the thermal or chemical stress applied to the cells. 4-PBA is an approved orphan drug, which has been shown to inhibit protein aggregation and thus ameliorate disorders associated with this phenomenon [16]. Thus, targeting the keratin IF aggregates with 4-PBA seemed a promising approach, and we therefore analyzed its effect on our KRT5mut and KRT14mut cell lines in different dosages.

We identified contrasting effects of 4-PBA treatment on EBS cells. Although 4-PBA reduced IF aggregates at a dose of 1 mM, it negatively impacted keratinocyte adhesion. The effect of thermal and chemical stress on aggregate formation was more pronounced in KRT14mut than KRT5mut cells, as was also the disruptive effect of 4-PBA on cell-cell and cell-ECM adhesion. The cell-cell contacts were disturbed in 4-PBA treated cells regarding localization and abundance of the desmosomal and adherence junction proteins. The cells employed compensatory mechanisms to overcome the diminished adhesion, e.g. by upregulating the focal adhesion integrin β1 and laminin-332, a pivotal adhesion ligand for keratinocytes. This was associated with increased proliferation and reduced migration of the cells.

Taken together, there were some effects of 4-PBA that both EBS cells had in common: reduction of aggregates, reduction of cell-cell adhesion (as shown by the dispase-dissociation assay and the reduced cell-cell contacts in stainings and immunoblots) and reduction in inflammatory markers. 4-PBA treatment had a greater negative impact on keratinocyte migration and cell-matrix adhesion of the KRT14mut than the KRT5mut cells. On the other side, increase in proliferation and its associated molecules in skin, e.g. KRT6 was observed significantly more in KRT5mut cells. These differences can probably be attributed to 2 major points: a) the KRT14mut cells had more aggregates already at resting state than the KRT5mut, and b) although these proteins form very stable subunits, their functions might be disparate e.g. regarding their role in keratinocyte survival and proliferation. One could only speculate that the aggregate production in the EBS cells is part of a compensatory mechanism of the cells, which results in enhanced cell-matrix adhesion. The aggregate reduction impacts more the KRT14mut cells, which had more aggregates to begin with, probably explaining the greater effects in adhesion. It might be that different compounds would be required to stabilize the cytoskeleton in

**Fig. 3.** Cell-ECM interactions are disturbed with enhanced focal adhesions after 1 mM 4-PBA treatment in NHK and EBS cells. A For the keratinocyte adhesion assay, the cells were coated on collagen I or left on untreated plates. We refer to the adhesion of the untreated cells on collagen I as 100% adhesion. After 4-PBA treatment, the adhesion of NHK appeared unchanged, whereas significant effects were found in 4-PBA-treated KRT14mut and less in KRT5mut cells [for KRT14mut + $^{*}P = .0411$ and for KRT5mut + $P = .3267$, student's t-test]. B Reduction of the fraction of adherent cells in NHK and EBS cells in the spinning disk assay after treatment with 1 mM 4-PBA [NHK+ $P = .4296$; KRT14mut + $P = .0652$; KRT5mut + $P = .6818$]. The effect of 4-PBA on adhesiveness is significant, with NHK and EBS cells taken together (All cells vs all cells+: $^{*}P = .0001$, student's t-test). C The focal adhesion-associated molecule integrin β1 (green) was stained and found greatly enhanced after 1 mM 4-PBA treatment especially in control and KRT5-mutated cells. Scale: 200 μm. D 4-PBA treatment resulted in altered staining of the epidermal F-actin cytoskeleton in control and EBS keratinocytes, whereas the total amount of F-actin was unchanged, as shown by immunoblotting, suggesting altered distribution of the actin filaments in the cells [for KRT14mut + $P = .9092$ and for KRT5mut + $P = .1796$, student's *t*-test]. Scale bar: 50 μm. The IF stainings were done in triplicates with at least 2 different cell lines for each group, before and after 4-PBA treatment. Shown are representative results from one experiment. E Immunoblotting for laminin-332 revealed increased amounts in cell lysates after 1 mM 4-PBA treatment. Bar graphs on the right show expression of laminin-332 normalized to tubulin as percentage of expression in untreated cells. Values represent mean ± S.E.M., paired t-test was used; for NHK $P = .6097$, for KRT14mut $P = .4084$ and for KRT5mut $P = .6291$.

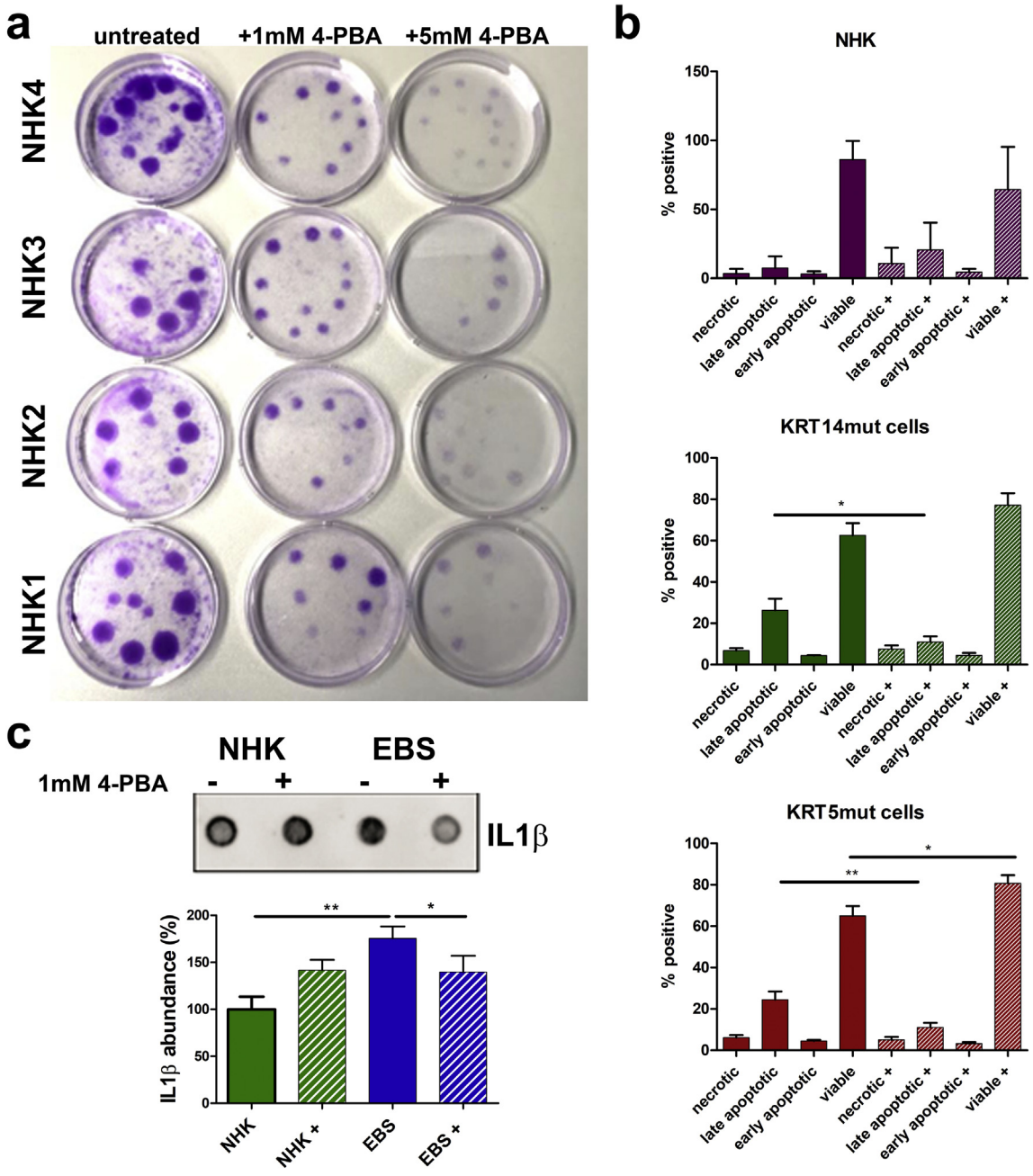


**Fig. 4.** Effects of 1 mM 4-PBA on cell apoptosis and IL1β expression. A. Colony-forming efficiency assay of 4 different primary NHKs, treated with different dosages of 4-PBA for 1 week is shown (untreated, 1 mM and 5 mM 4-PBA every 2 days). The 4-PBA-treated cells had a clearly reduced growth potential compared to untreated keratinocytes, as visualized by the colony size. Colony size decreased with increasing 4-PBA dosage. B Cells were stained with annexin V / DAPI and then visualized with flow cytometry to detect apoptotic cells. The experiment was done in triplicates with 2 different cell lines for each group. Bar graphs of all experiments show clearly increased numbers of apoptotic cells (especially late apoptotic) in the EBS keratinocyte cell lines compared to NHK; irrespective of the underlying keratin mutations (differences in NHK versus NHK+ [+ standing for cells treated with 1 mM 4-PBA]: necrotic cells $P = .1061$, late apoptotic cells $P = .0955$, early apoptotic cells $P = .1946$ and viable cells $P = .0817$; differences in KRT14mut versus KRT14mut+: necrotic cells $P = .7449$, late apoptotic cells $^{*}P = .0249$, early apoptotic cells $P = .9868$ and viable cells $P = .0979$; differences in KRT5mut versus KRT5mut+: necrotic cells $P = .5548$, late apoptotic cells $^{**}P = .0097$, early apoptotic cells $P = .1967$ and viable cells $^{*}P = .0211$). Thus, 4-PBA treatment had different effects in NHK and EBS cells. In NHK it induced apoptosis, whereas in the EBS cells it reversed apoptosis. Values represent mean ± S.E.M., unpaired *t*-test was used. C Total IL1β abundance was evaluated by dot blots in untreated NHK and EBS and 4-PBA treated cells. For the experiment two NHK, two KRT14mut and two KRT5mut cells were used, before and after treatment with 1 mM 4-PBA were used. The experiment was performed in triplicates. The data of the KRT14mut and KRT5mut cells were pulled together for the statistical analysis, since they were similar. Shown above is a representative picture of one NHK and one KRT5mut cell line, before and after 4-PBA treatment. IL1β expression was higher in EBS cells compared to NHK prior to 1 mM 4-PBA treatment, whereas after treatment, IL1β expression was lower in EBS cells compared to NHK cells. Values represent mean ± S.E.M., unpaired t-test was used; for NHK versus EBS $^{**}P = .0096$, for EBS+ 1 mM 4-PBA $^{*}P = .0257$.

KRT14mut and KRT5mut cells. Nonetheless, our data clearly highlight that the aggregate reduction is by itself not sufficient to stabilize the cytoskeleton.

Using the current conditions, 4-PBA represents not a viable treatment option for EBS, however, lower concentrations of 4-PBA in combination with anti-inflammatory drugs may act more selectively against aggregated keratins. In addition, other drugs targeting the aggregate formation are definitely worth being investigated for their effects at a cellular and tissue level. Keratin aggregates can induce inflammation [43,44]. Our results indicate that 4-PBA treatment reduced not only cellular aggregates, but also apoptosis of EBS cells and IL1β secretion. In a similar manner, protein misfolding induces cellular stress and promotes

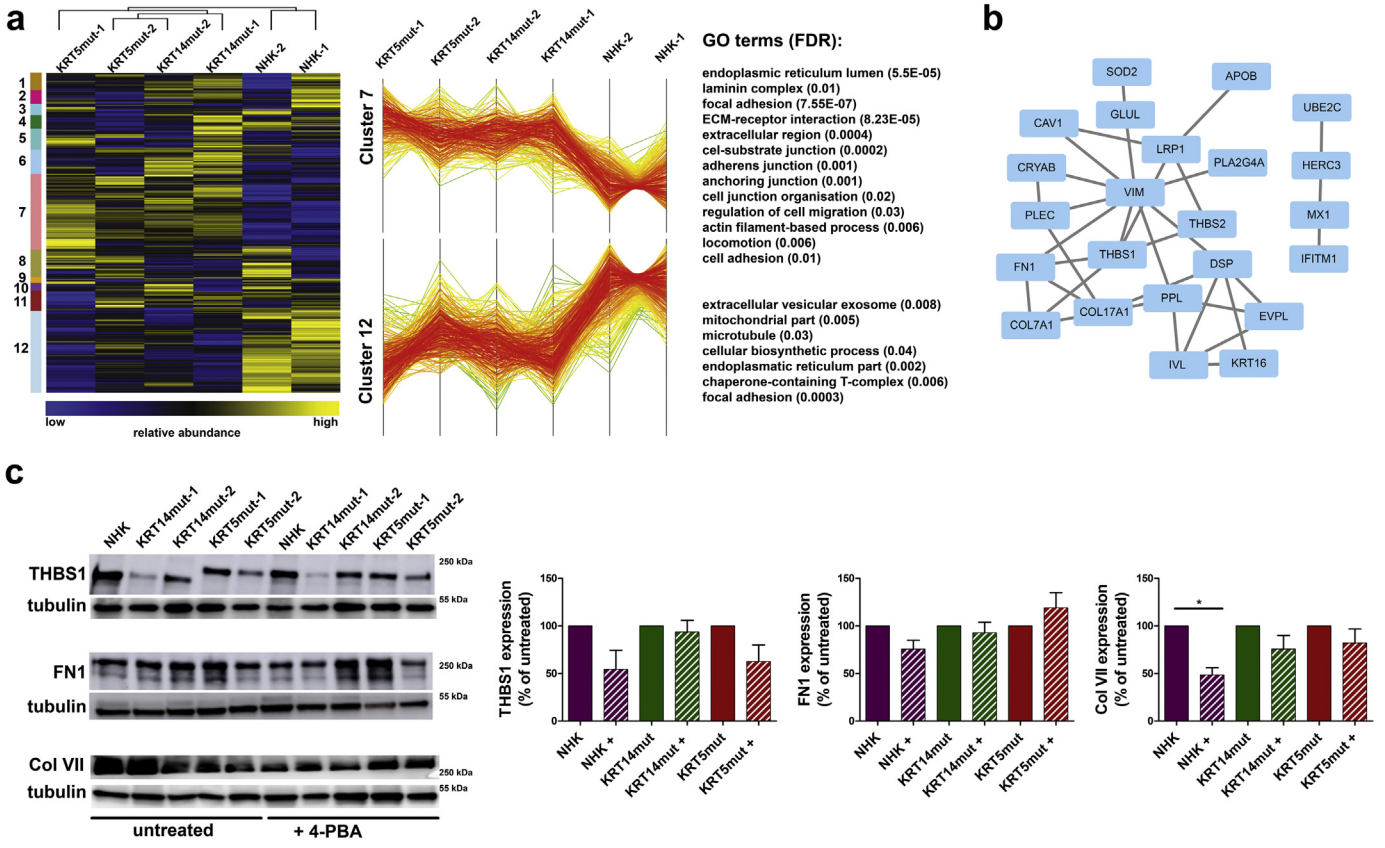


**Fig. 5.** Proteomics reveals effects of 4-PBA treatment on extracellular matrix and cytoskeleton proteins. A Heat map of hierarchically clustered protein abundance ratios comparing 4-PBA-treated cells. SILAC ratios were log2-transformed and normalized (z-score). Samples and protein ratios were clustered hierarchically. On the left, the different clusters are shown. Clusters 7 and 12 are differentially regulated in NHK versus EBS cells. On the right, the GO terms enriched in each Cluster are shown. B Proteins that were significantly affected by 4-PBA treatment in minimally one of the samples (Significance A, $p < .05$, BH corrected) carrying GO terms related to extracellular matrix and cytoskeleton were short-listed and analyzed on potential interactions using default settings in STRING DB. C Western blot analysis to test the identified targets shows reduced expression of thrombospondin 1 (THBS1), fibronectin 1 (FN1) and collagen VII (Col VII). Bar graphs on the right show the quantification of 3 subsequent experiments done with 2 different EBS cell lines. Shown are the mean ± S.E.M. of the normalized protein abundance. Paired t-test was used to calculate significance [THBS1: for NHK $P = .1497$, for KRT14mut $P = .6293$ and for KRT5mut $P = .0947$; FN1: for NHK $P = .1180$, for KRT14mut $P = .5414$ and for KRT5mut $P = .2840$; ColVII: for NHK *P = .0211, for KRT14mut $P = .1498$ and for KRT5mut $P = .2911$].

(auto)inflammation [45]. Thus, the role of inflammation as disease determinant in EBS deserves a closer look.

We employed unbiased global proteomics to connect the observed changes on a cellular level to molecular events. Analysis of EBS and control keratinocytes after 1 mM 4-PBA treatment uncovered reduced abundance of ECM proteins and proteins of the cytoskeleton, however, this failed to enhance cell-cell and cell-matrix adhesion which are crucial in skin fragility disorders. The reduction of E-cadherin is possibly a central event, since loss of cadherin-mediated adhesion is associated with increased Wnt signaling through β-catenin and co-induction of the NF-κB pathway. Actin cytoskeleton disruption has been linked to NF-κB activation [46]. In addition, loss of another adherence junction protein, p120-catenin, has been shown to be associated with activated NF-κB, as an intrinsic response to loss of p120 rather than extrinsic consequence of inflammation [47]. In our cells, this activation was combined with increased cell proliferation and enhanced TNF-α expression, contrasting the observed IL1β reduction and reflecting how complex the induction of such central pathways as NF-κB, is. We postulate that the reduced IL1β levels are directly linked to the loss of the aggregates in the cell, whereas increased TNF-α reflects a secondary event to NF-κB and Wnt signaling activation.

Taken together, we show that low dose 4-PBA has some favorable effects on EBS cells. What our data make clear though is that higher doses of 4-PBA are toxic for keratinocytes, thus the drug should be avoided in skin fragility disorders. Other molecular chaperones targeting aggregate formation and ER stress could represent possible therapeutic tools, however their effects on cellular adhesion and migration must first be carefully investigated.

## 4. Material and methods

### 4.1. Clinical samples and cell culture

EBS diagnosis was based on clinical assessment, morphological analysis of skin biopsies and finally mutation analysis. After informed consent, skin biopsies and ethylenediaminetetraacetic acid (EDTA) blood was obtained from the patients for diagnostic purposes. The project was approved by the ethics committee of the University of Freiburg and was conducted according to the Declaration of Helsinki principles. Skin samples from EBS patients and from healthy individuals who underwent surgery were used after informed written consent for immunostainings and isolation of keratinocytes. Primary keratinocytes from patients' and control skin were cultured in serum-free keratinocyte medium supplemented with 25 μg/ml bovine pituitary extract and 0.2 ng/ml recombinant epidermal growth factor (Invitrogen, Darmstadt, Germany) using standard methods (Kiritsi et al., 2011). The immortalization was performed after co-transfection of the cells with the HPV18 E6 and E7 genes (pLenti-III-HPV-16 E6/E7 lentivector, ABM, Richmond, Canada), as described before [48].

### 4.2. Cell treatments

Cell treatments were performed in six-well plates, with 0.3 to $0.4 \times 10^6$ cells seeded the day before treatment and incubated overnight at 37 °C and 5% $CO^2$. 4-PBA (Sigma-Aldrich), a chemical chaperone, was used at a concentration of 1 and 10 mM for 24 or 48 h. For inhibition of

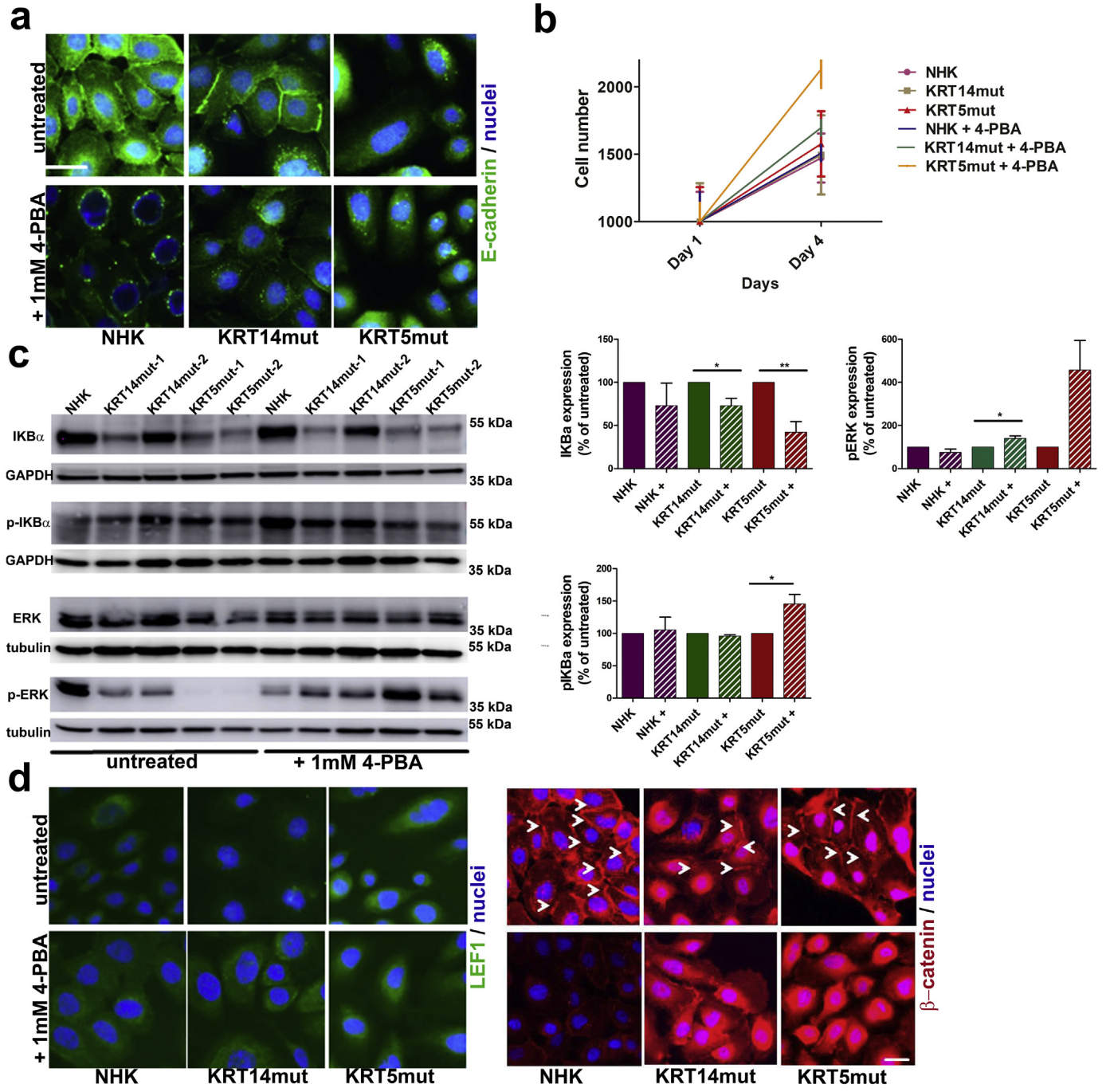


**Fig. 6.** 4-PBA treatment co-induces the NF-κB and the Wnt signaling pathways in EBS cells. A Immunofluorescence staining with E-cadherin (green) was reduced after 4-PBA treatment; in addition, some round vesicles around the nucleus were present in all cell lines as an indication of perinuclear accumulation of E-cadherin. Scale bar: 50 μm. B Cell proliferation was enhanced in all cell lines after 1 mM 4-PBA treatment. C Immunoblotting for IKBα showed reduced levels in EBS cells compared to NHK before treatment, although there was some variation between the KRT14mut cell lines. After 4-PBA treatment, IKBα decreased even more [for NHK $P = .4113$, for KRT14mut $^{*}P = .0275$ and for KRT5mut $^{**}P = .0094$]. Phosphorylated IKBα (pIKBα) was enhanced after 4-PBA treatment in the KRT5mut cells [for NHK $P = .8099$, for KRT14mut $P = .1041$ and for KRT5mut $^{*}P = .0257$]. Phosphorylated ERK (pERK) was significantly enhanced in the EBS cell lines [for NHK $P = .2128$, for KRT14mut $^{*}P = .0133$ and for KRT5mut $^{*}P = .0409$]. Bar graphs on the right show the quantification of 3 subsequent experiments. Shown are the mean ± S.E.M. of the normalized protein abundance. Paired t-test was used to calculate significance. D Staining for the lymphoid enhancer factor (LEF1) (green, left panel) is enhanced after 4-PBA treatment in all cell lines. Immunofluorescence staining for β-catenin (red, right panel) demonstrating adherence junctions appears enhanced and more diffuse after 4-PBA treatment in the EBS cells (arrows point to the cell-cell contacts, which seem diminished after 4-PBA). Scale bar: 50 μm.

the proteasome, the cells were incubated with 100 μM MG-132 (Calbiochem, Darmstadt, Germany) for 6 h.

### 4.3. Immunoblot analysis

Immunoblot analysis was performed as described before [13,49] using primary antibodies to desmoplakin, E-cadherin, β-catenin, plakoglobin, keratin 14, keratin 17, keratin 6, keratin 16, IKBα and phosphorylated- IKBα, ERK and phosphorylated-ERK, and tubulin to control loading (see Supplemental Table 2). For the analysis of IL-1β and Tnf-α, dot blots were performed. Blots were developed using ECL substrate (Thermo Scientific, Rockford, IL) and the Fusion SL system (Peqlab, Erlangen, Germany). The signals obtained from Western blot analyses were densitometrically quantified with ImageJ's gel analysis

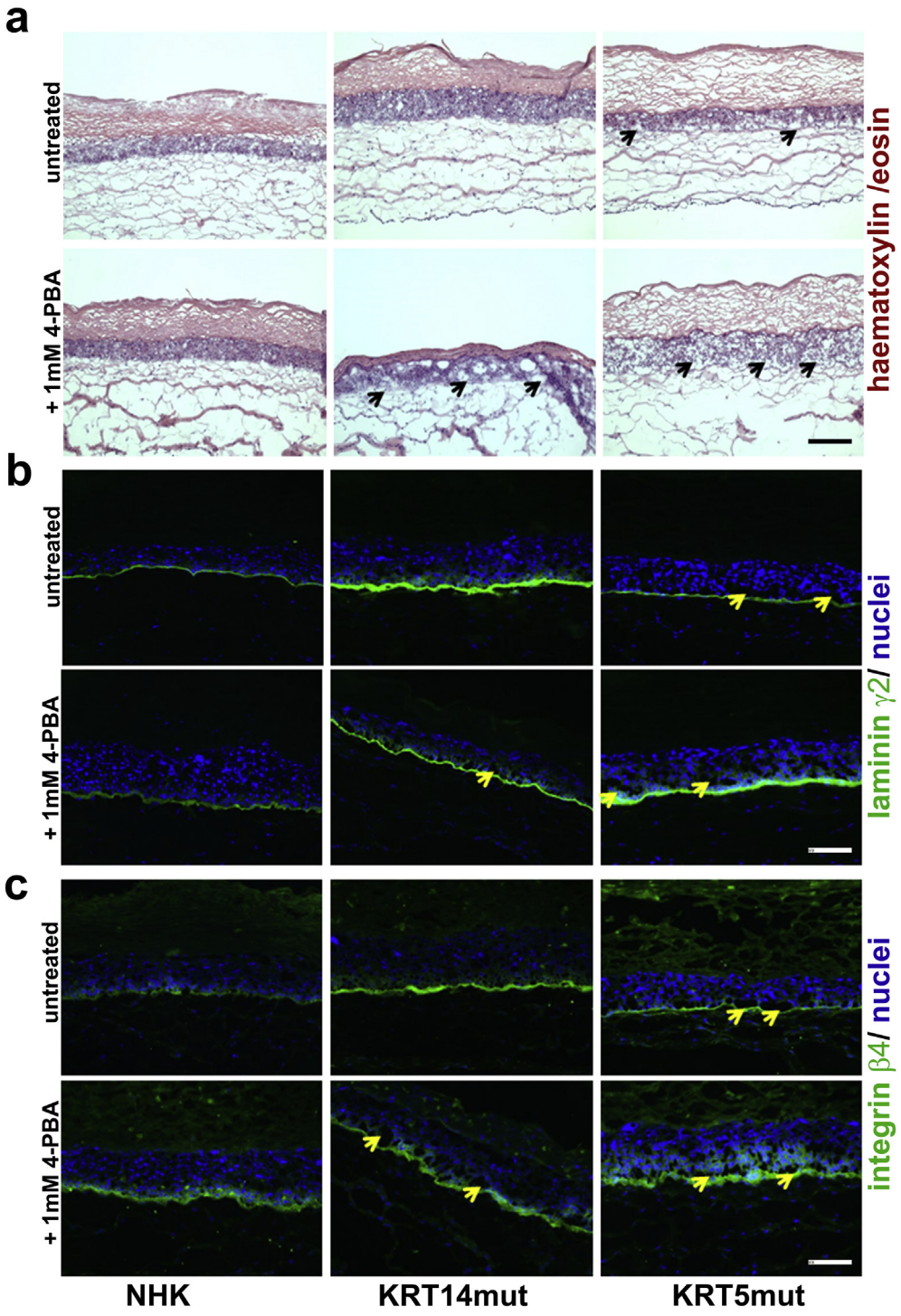


**Fig. 7.** Skin equivalents with NHK and EBS cells show several intra- and subepidermal splits after 1 mM 4-PBA treatment, as well as perturbed staining patterns of laminin-332 and of integrin β4. A Skin equivalents with control vs EBS keratinocytes for the epidermal part and control normal human fibroblasts for the dermal part were employed to assess the effect of 4-PBA in a 3D model. Only a few areas of dermo-epidermal detachment are present in the EBS skin equivalents compared to the control skin equivalents, as shown with haematoxylin/ eosin staining. In the 4-PBA treated skin, however, several intra- and subepidermal splits (black arrows) were found, corroborating the adhesion defect. Scale: 100 μm. B Laminin-332 deposition was irregular and patchy in the NHK, whereas it also stained the suprabasal keratinocytes in the EBS cells. In the 4-PBA treated skin, again, several intra- and subepidermal splits (yellow arrows) were observed. Scale: 100 μm. C Integrin β4 showed also an irregular and more pronounced, patchy, suprabasal expression in the treated skin equivalents. Thus, 4-PBA treatment perturbs laminin-332 organization, which in turn seems to abrogate strictly polarized expression of integrin α6β4 in basal keratinocytes. The yellow arrows depict intra- and subepidermal splits, present mostly in the 4-PBA treated skin. Scale: 100 μm.

program, values were expressed as percentage of expression levels seen in untreated cells after normalization to loading control.

### 4.4. Indirect immunofluorescence staining

Cells were seeded on uncoated coverslips and allowed to grow for two days, fixed and processed as described [50]. Before fixing the cells, they were switched to media containing 1.2 mM $Ca^{2+}$ for 24 h. Primary antibodies used in this study were the following: keratin 5, plectin, desmoplakin, E-cadherin, phalloidin, integrin β1, β-catenin, plakoglobin (see Supplemental Table 2). Nuclei were visualized with DAPI. As secondary antibodies, Alexa anti-rabbit IgG, anti-guinea pig IgG and anti-mouse IgG (Invitrogen) were used. Images were captured by immunofluorescence microscopy (Zeiss Axio Imager, Zeiss, Germany). The software ImageJ was applied for quantification, and GraphPad Prism for statistical analyses.

### 4.5. Dispase-based dissociation assay

Control and EBS cells were seeded in triplicates; 24 h after reaching confluence, the cells were treated with 1.2 mM $Ca^2$ overnight. The cultures were washed twice in Dulbecco's PBS (DPBS) and then incubated in 1 mg/ml dispase for 30 min. Phase-contrast images were taken before and after dispase digestion. The released monolayers were washed twice with DPBS and transferred to 15 ml conical tubes. The tubes were secured to a rocker and subjected to 50 inversion cycles. The fragments were counted using an inverted microscope.

### 4.6. Spinning disk method

The spinning disk consists of a stationary plate (petri dish) and a rotating glass plate driven by air pressure [26]. The applied shear stress depends on the rotation frequency of the spinning plate, the distance between rotational and stationary plate, and the viscosity of the cell culture medium. In these experiments we used a rotational frequency of 1500 rpm and a plate distance of 150 μm. We seeded 15.000 cells per well and cell line in 1.5 ml medium for 24 h. Cell nuclei where stained with Hoechst dye prior to fluid shear stress application. Images of the cells (both in brightfield and fluorescent mode) were taken before and after 5 min of stress application. A series of images were recorded, starting from the middle of the dish and then 10 field of views radially outwards (x-direction). We also recorded adjacent 3 fields of views for each x-position going in the y-direction. For evaluating the fraction of attached cells, we used the program “Clickpoints” [51] to count the cells in a region between 2 and 4 mm distance from the dish center, where the shear stress was between 7 and 15 dyn/cm^2 (0,7 to 1,5 Pa).

### 4.7. Migration, proliferation and cell adhesion assays

To investigate the migration of the keratinocytes, an in vitro wound closure assay was performed. The keratinocytes were cultured to confluency on Ibidi μ-dishes with culture-inserts. After removal of the inserts, the cells were rinsed with PBS and incubated further in culture medium under 5% $CO_2$ at 37 °C in a Nikon Biostation immunofluorescence microscope (Nikon Instruments Inc., Melville, NY). Photographs were captured every 60 min for 24 h and the wound areas were measured using the Image J software. For assessment of proliferation, keratinocytes were seeded on micro plates with a local ionic electrode interface. The cells were monitored over the course of at least 4 days. For the cell adhesion assay tissue culture wells were coated with 10 ng/ml of collagen I (Sigma-Aldrich, Munich, Germany) or left on untreated plates at 4 °C overnight. After saturation with 1% BSA, equal numbers of cells were seeded. The keratinocytes adhered for 1 h at 37 °C, then were fixed with ethanol and stained with 0.5% crystal violet for 15 min. Adherent cells were photographed and quantified by measuring the optical density at 540 nm.

### 4.8. Colony-forming assay

Around 1000 cells from primary normal human keratinocytes were seeded on 6 cm tissue cultures dishes. They were incubated for 7 days with 1 mM or 10 mM 4-PBA on 37 °C, 5% CO2. Media were changed every 2 days. The cells were fixed with formalin / PBS for 15 min at room temperature. After washing with PBS, they were stained with 0,05% crystal violet in PBS, after incubation for 1 h at room temperature.

### 4.9. Organotypic skin equivalents

3D organotypic co-cultures were prepared as described before [52] to evaluate the effects of 4-PBA treatment on cell adhesion. The co-cultures were constructed with control human or KRT5- or KRT14-mutated keratinocytes as epithelial cells and normal human fibroblasts, forming a skin-like bilayered structure. 4-PBA was given with every medium change at a dosage of 1 mM in the cell medium.

### 4.10. Software for classification of the cells

For counting and classifying cells grown on a coverslip into cells with or without aggregates after immunofluorescence staining, custom programs written in Matlab and Python were used. After defining a starting position on the coverslip, a 10 × 10 grid of images with an overlap of 10% in x and y direction was recorded using a 63× oil objective of an inverse immunofluorescence microscope (Leica DMI6000 CS). At every position, a stack of 31 z-slices (0.5 μm z-distance) was recorded, which was joined using a maximum sharpness projection. Afterwards, a single composite image was stitched using the stitching plugin of ImageJ. To improve the visual appearance of the large stitched image, the median intensity was subtracted and the contrast maximized. Using ClickPoints software [51], cells were then manually labeled in two categories: cells without aggregates and cells with aggregates. The evaluation of a large region on the coverslip helps to reduce bias, which could be introduced by manually selecting only a few fields of view for analysis.

### 4.11. Annexin V binding assay

Adherent keratinocytes were dissociated from the culture plate by trypsinization and placed as suspension in a 96-well round bottom plate (around 100.000 cells per well), washed twice with PBS and stained with Annexin V as indicated in the manufacturer's datasheet (Becton-Dickinson). As positive controls, cells treated overnight with staurosporine (1 μM) or heat treated cells were used. Necrotic cells were stained by addition of DAPI directly before analysis of annexin-V positive apoptotic cells by flow cytometry. The experiment was performed with 2 different cell lines for each category (NHK, KRT14mut, KRT5mut) and then repeated 3 times.

### 4.12. Mass spectrometry (MS) analysis

For MS analysis, cells were cultured in keratinocyte growth medium (KGM2) (Promocell, Heidelberg, Germany) without arginine and lysine, but with “SupplementMix” (0.004 ml/ml bovine pituitary gland extract, 0.125 ng/ml recombinant human epidermal growth factor, 5 μg/ml recombinant human insulin, 0.33 μg/ml hydrocortisone, 0.39 μg/ml epinephrine, 10 μg/ml human holo transferrin) and 0.06 mM CaCl2, 210 mg/l L-arginine and 63 mg/l L-lysine for the unlabeled condition. Cells were “heavy” labeled for 2 weeks with 210 mg/l L-arginine-13C6-15 N4 (Arg10) and 63 mg/l L-lysine-13C6-15 N2 (Lys8) or “medium-heavy” labeled with 210 mg/l L-arginine-13C6 (Arg6) and 63 mg/l L-lysine-2H4 (Lys4)31.

Cells were harvested, mixed 1:1:1 on protein level and lysates were taken up in SDS-PAGE loading buffer. 1 mM DTT was used for reduction

(5 min at 95 °C) and 5.5 mM iodoacetamide for alkylation (30 min at RT). Mixed samples were separated on gradient gels of 4–12%. Gel lanes were cut into 10 slices each, proteins therein were digested with trypsin and the resulting peptide mixtures were processed on STAGE tips and analyzed by LC-MS/MS as described51.

MS measurements were performed on an LTQ Orbitrap XL mass spectrometer, which was coupled to an Easy nanoLC. Fused silica HPLC–column tips (20 cm length, 75 μm i.d.) were packed with Reprosil–Pur 120 C18-AQ, 1.9 μm (Dr. Maisch). Samples were loaded on the column. A gradient of A (0.1% formic acid in water) and B (0.1% formic acid in 80% acetonitrile in water) was used for peptide separation (loading of sample with 0% B; separation ramp: from 5 to 30% B within 85 min). The flow rate was set to 250 nL/min; for sample application it was 600 nL/min. The mass spectrometer operated data–dependently switching automatically between MS (max. of $1 \times 106$ ions) and MS/MS. Each full scan was followed by a maximum of five tandem MS scans in the linear ion trap (normalized collision energy of 35%; target value 5000). Singly charged parent ions and ions with an unassigned charge state were excluded for fragmentation. The MS mass range was $m/z = 370–2000$. Resolution was set to 60,000. MS parameters: no sheath and auxiliary gas flow; spray voltage 2.3 kV; ion–transfer tube temperature 125 °C.

MS files were processed by MaxQuant (version 1.4.1.2), which performs peak detection, generation of peak lists, and database searches using a full-length UniProt human forward-reverse database extended with common contaminants such as enzymes used for in–gel digestion52. Carbamidomethylcysteine was set as fixed modification and protein amino–terminal acetylation and oxidation of methionine were set as variable modifications. The quantitation mode was set to triple SILAC. Missed cleavages was set to three, enzyme specificity was trypsin/P, mass tolerance was 20 ppm for first search, and MS/MS tolerance was 0.5 Da. After recalibration, average mass precision of identified peptides was <1 ppm. Peptide identification and relative quantification of proteins was performed using following criteria: 2 min 'match-between-run', 0.01 peptide and protein FDRs, minimum peptide length of 6, minimum number of peptides for identification and quantitation of proteins of 1 unique, minimum ratio count 2. Identified proteins were re-quantified.

### *4.13. Statistical analysis*

The GraphPad Prism 5.03 software was used for statistical analysis, and data were analyzed using paired or unpaired Student's *t*-test with Welch correction, where appropriate. The statistical analysis of the dynamic disassembly of the keratin IF networks, was based on the assessment of 150 cells of each keratinocyte cell line, which were manually photographed from different optical fields and afterwards classified into cells with or cells without aggregates.

Supplementary data to this article can be found online at https://doi.org/10.1016/j.ebiom.2019.04.062.

## Funding

This work was supported by the EB research partnership and the Mathilde-Wagner-Habilitationspreis to DK, by the German Research Foundation DFG [grant DE 1757/3-2 to JD, ES 431/1-1 to PRE, and FA 336/8-1 to MS and BF].

## Acknowledgments

We acknowledge the expert technical assistance of Käthe Thoma. We also acknowledge the contribution of Prof. Jürgen Kohlhase, Humangenetik Freiburg for identifying the *KRT5* and *KRT14* mutations and thus confirming the EBS diagnosis in the patients presented here.

## Author contributions

MS, AP, RCT, AS, RG, IT and LW were involved in experimentation and data analysis; PRE, MH and IA were both involved in experimentation and data acquisition, PRE also in data analysis; AN was involved in experimentation, data analysis and data interpretation; LBT, TM, BF, RS and JD were involved in the analysis and interpretation of the data; RG, AS and BF developed the spinning disk assay and wrote the custom programs for data analysis; RS conceived the study together with DK and was involved in data analysis / interpretation and writing of the article; DK was involved in project coordination, data acquisition, analysis and interpretation, and wrote the first version of the article.

## Conflicts of interest

No conflict of interest to declare.

## References

[1] Pfendner EG, Bruckner AL. Epidermolysis bullosa simplex. In: Pagon RA, Adam MP, Ardinger HH, Wallace SE, Amemiya A, Bean LJH, et al, editors. GeneReviews(®). Seattle (WA): University of Washington, Seattle; 1993 Internet.
[2] Lee C-H, Coulombe PA. Self-organization of keratin intermediate filaments into cross-linked networks. J Cell Biol 2009;186(3):409–21 10 August.
[3] Chamcheu JC, Navsaria H, Pihl-Lundin I, Liovic M, Vahlquist A, Torma H. Chemical chaperones protect epidermolysis bullosa simplex keratinocytes from heat stress-induced keratin aggregation: involvement of heat shock proteins and MAP kinases. J Invest Dermatol 2011;131(8):1684–91 August.
[4] Zomer HD, Trentin AG. Skin wound healing in humans and mice: challenges in translational research. J Dermatol Sci 2018;90(1):3–12 April.
[5] Vijayaraj P, Söhl G, Magin TM. Keratin transgenic and knockout mice: functional analysis and validation of disease-causing mutations. Methods Mol Biol Clifton NJ 2007;360:203–51.
[6] Werner NS, Windoffer R, Strnad P, Grund C, Leube RE, Magin TM. Epidermolysis bullosa simplex-type mutations alter the dynamics of the keratin cytoskeleton and reveal a contribution of actin to the transport of keratin subunits. Mol Biol Cell März, 2004;15(3):990–1002.
[7] Tan TS, Ng YZ, Badowski C, Dang T, Common JE, Lacina L, et al. Assays to study consequences of cytoplasmic intermediate filament mutations: the case of epidermal keratins. Methods Enzymol 2016;568:219–53.
[8] Liovic M, Lee B, Tomic-Canic M, D'Alessandro M, Bolshakov VN, Lane EB. Dual-specificity phosphatases in the hypo-osmotic stress response of keratin-defective epithelial cell lines. Exp Cell Res 2008;314(10):2066–75 10 Juni.
[9] Chamcheu JC, Lorié EP, Akgul B, Bannbers E, Virtanen M, Gammon L, et al. Characterization of immortalized human epidermolysis bullosa simplex (KRT5) cell lines: trimethylamine N-oxide protects the keratin cytoskeleton against disruptive stress condition. J Dermatol Sci März, 2009;53(3):198–206.
[10] Russell D, Ross H, Lane EB. ERK involvement in resistance to apoptosis in keratinocytes with mutant keratin. J Invest Dermatol März, 2010;130(3):671–81.
[11] D'Alessandro M, Russell D, Morley SM, Davies AM, Lane EB. Keratin mutations of epidermolysis bullosa simplex alter the kinetics of stress response to osmotic shock. J Cell Sci 2002;115(Pt 22):4341–51 15 November.
[12] Morley SM, D'Alessandro M, Sexton C, Rugg EL, Navsaria H, Shemanko CS, et al. Generation and characterization of epidermolysis bullosa simplex cell lines: scratch assays show faster migration with disruptive keratin mutations. Br J Dermatol 2003;149(1):46–58 Juli.
[13] Homberg M, Ramms L, Schwarz N, Dreissen G, Leube RE, Merkel R, et al. Distinct impact of two keratin mutations causing epidermolysis bullosa simplex on keratinocyte adhesion and stiffness. J Invest Dermatol 2015;135(10):2437–45 Oktober.
[14] Qi X, Hosoi T, Okuma Y, Kaneko M, Nomura Y. Sodium 4-phenylbutyrate protects against cerebral ischemic injury. Mol Pharmacol 2004;66(4):899–908 Oktober.
[15] Liu S-H, Yang C-C, Chan D-C, Wu C-T, Chen L-P, Huang J-W, et al. Chemical chaperon 4-phenylbutyrate protects against the endoplasmic reticulum stress-mediated renal fibrosis in vivo and in vitro. Oncotarget 2016;7(16):22116–27 19 April.
[16] Winter L, Staszewska I, Mihailovska E, Fischer I, Goldmann WH, Schroder R, et al. Chemical chaperone ameliorates pathological protein aggregation in plectin-deficient muscle. J Clin Invest 2014;124(3):1144–57 März.
[17] Lee CS, Hanna AD, Wang H, Dagnino-Acosta A, Joshi AD, Knoblauch M, et al. A chemical chaperone improves muscle function in mice with a RyR1 mutation. Nat Commun 24 März, 2017;8:14659.
[18] Zhou W, Bercury K, Cummiskey J, Luong N, Lebin J, Freed CR. Phenylbutyrate up-regulates the DJ-1 protein and protects neurons in cell culture and in animal models of Parkinson disease. J Biol Chem 29 April, 2011;286(17):14941–51.
[19] Maier K, He Y, Esser PR, Thriene K, Sarca D, Kohlhase J. u. a. single amino acid deletion in Kindlin-1 results in partial protein degradation which can be rescued by chaperone treatment. J Invest Dermatol 2016;136(5):920–9.
[20] Chamcheu JC, Pihl-Lundin I, Mouyobo CE, Gester T, Virtanen M, Moustakas A, et al. Immortalized keratinocytes derived from patients with epidermolytic ichthyosis reproduce the disease phenotype: a useful in vitro model for testing new treatments. Br J Dermatol Februar, 2011;164(2):263–72.

[21] Naoi S, Hayashi H, Inoue T, Tanikawa K, Igarashi K, Nagasaka H, et al. Improved liver function and relieved pruritus after 4-phenylbutyrate therapy in a patient with progressive familial intrahepatic cholestasis type 2. J Pediatr Mai, 2014;164(5):1219–27 [e3].
[22] Strnad P, Windoffer R, Leube RE. In vivo detection of cytokeratin filament network breakdown in cells treated with the phosphatase inhibitor okadaic acid. Cell Tissue Res 2001;306(2):277–93 November.
[23] Osmanagic-Myers S, Gregor M, Walko G, Burgstaller G, Reipert S, Wiche G. Plectin-controlled keratin cytoarchitecture affects MAP kinases involved in cellular stress response and migration. J Cell Biol 14 August, 2006;174(4):557–68.
[24] Wong P, Coulombe PA. Loss of keratin 6 (K6) proteins reveals a function for intermediate filaments during wound repair. J Cell Biol 27 Oktober, 2003;163(2):327–37.
[25] Rousselle P, Montmasson M, Garnier C. Extracellular matrix contribution to skin wound re-epithelialization. Matrix Biol 10 Januar, 2018;75-76:12–26.
[26] Schilling A. A novel live imaging spinning disk device for adhesion strength measurements on Mg substrates Erlangen; 2013.
[27] Nishimura M, Nishie W, Shirafuji Y, Shinkuma S, Natsuga K, Nakamura H, et al. Extracellular cleavage of collagen XVII is essential for correct cutaneous basement membrane formation. Hum Mol Genet 15 Januar, 2016;25(2):328–39.
[28] Arrasate M, Finkbeiner S. Protein aggregates in Huntington's disease. Exp Neurol 2012;238(1):1–11 November.
[29] Yoneda K, Furukawa T, Zheng Y-J, Momoi T, Izawa I, Inagaki M, et al. An autocrine/paracrine loop linking keratin 14 aggregates to tumor necrosis factor alpha-mediated cytotoxicity in a keratinocyte model of epidermolysis bullosa simplex. J Biol Chem 20 Februar, 2004;279(8):7296–303.
[30] El-Hawary MS, Abdel-Halim MRE, Sayed SS, Abdelkader HA. Apocytolysis, a proposed mechanism of blister formation in epidermolysis bullosa simplex. Arch Dermatol Res Mai, 2015;307(4):371–7.
[31] Yamanaka K, Tanaka M, Tsutsui H, Kupper TS, Asahi K, Okamura H, et al. Skin-specific caspase-1-transgenic mice show cutaneous apoptosis and pre-endotoxin shock condition with a high serum level of IL-18. J Immunol Baltim Md 1950 15 Juli, 2000;165(2):997–1003.
[32] Wally V, Lettner T, Peking P, Peckl-Schmid D, Murauer EM, Hainzl S, et al. The pathogenetic role of IL-1β in severe epidermolysis bullosa simplex. J Invest Dermatol Juli, 2013;133(7):1901–3.
[33] Thriene K, Grüning BA, Bornert O, Erxleben A, Leppert J, Athanasiou I, et al. Combinatorial omics analysis reveals perturbed lysosomal homeostasis in collagen VII-deficient keratinocytes. Mol Cell Proteomics MCP 11 Januar, 2018;17(4):565–79.
[34] Mattauch S, Sachs M, Behrens J. Liprin-α4 is a new hypoxia-inducible target gene required for maintenance of cell-cell contacts. Exp Cell Res 15 Oktober, 2010;316(17):2883–92.
[35] Hochrainer K, Pejanovic N, Olaseun VA, Zhang S, Iadecola C, Anrather J. The ubiquitin ligase HERC3 attenuates NF-κB-dependent transcription independently of its enzymatic activity by delivering the RelA subunit for degradation. Nucleic Acids Res 16 November, 2015;43(20):9889–904.
[36] Streicher KL, Willmarth NE, Garcia J, Boerner JL, Dewey TG, Ethier SP. Activation of a nuclear factor kappaB/interleukin-1 positive feedback loop by amphiregulin in human breast cancer cells. Mol Cancer Res MCR 2007;5(8):847–61 August.
[37] Cáceres LC, Bonacci GR, Sánchez MC, Chiabrando GA. Activated α(2) macroglobulin induces matrix metalloproteinase 9 expression by low-density lipoprotein receptor-related protein 1 through MAPK-ERK1/2 and NF-κB activation in macrophage-derived cell lines. J Cell Biochem 15 Oktober, 2010;111(3):607–17.
[38] Lin Y, Chen X-J, Liu W, Gong B, Xie J, Xiong J-H, et al. Two novel mutations on exon 8 and intron 65 of COL7A1 gene in two Chinese brothers result in recessive dystrophic epidermolysis bullosa. PloS One 2012;7(11):e50579.
[39] McDaniel DK, Eden K, Ringel VM, Allen IC. Emerging roles for noncanonical NF-κB signaling in the modulation of inflammatory bowel disease pathobiology. Inflamm Bowel Dis 2016;22(9):2265–79.
[40] Greten FR, Arkan MC, Bollrath J, Hsu L-C, Goode J, Miething C, et al. NF-kappaB is a negative regulator of IL-1beta secretion as revealed by genetic and pharmacological inhibition of IKKbeta. Cell 7 September, 2007;130(5):918–31.
[41] Ma B, Hottiger MO. Crosstalk between Wnt/β-catenin and NF-κB signaling pathway during inflammation. Front Immunol 2016;7:378.
[42] Hirsch T, Rothoeft T, Teig N, Bauer JW, Pellegrini G, De Rosa L, et al. Regeneration of the entire human epidermis using transgenic stem cells. Nature 16, 2017;551(7680):327–32.
[43] Fischer H, Langbein L, Reichelt J, Praetzel-Wunder S, Buchberger M, Ghannadan M, et al. Loss of keratin K2 expression causes aberrant aggregation of K10, hyperkeratosis, and inflammation. J Invest Dermatol Oktober, 2014;134(10):2579–88.
[44] Lu H, Chen J, Planko L, Zigrino P, Klein-Hitpass L, Magin TM. Induction of inflammatory cytokines by a keratin mutation and their repression by a small molecule in a mouse model for EBS. J Invest Dermatol Dezember, 2007;127(12):2781–9.
[45] Agyemang AF, Harrison SR, Siegel RM, McDermott MF. Protein misfolding and dysregulated protein homeostasis in autoinflammatory diseases and beyond. Semin Immunopathol Juli, 2015;37(4):335–47.
[46] Kustermans G, El Benna J, Piette J, Legrand-Poels S. Perturbation of actin dynamics induces NF-kappaB activation in myelomonocytic cells through an NADPH oxidase-dependent pathway. Biochem J 15 April, 2005;387(Pt 2):531–40.
[47] Perez-Moreno M, Davis MA, Wong E, Pasolli HA, Reynolds AB, Fuchs E. p120-catenin mediates inflammatory responses in the skin. Cell 10 Februar, 2006;124(3):631–44.
[48] Hawley-Nelson P, Vousden KH, Hubbert NL, Lowy DR, Schiller JT. HPV16 E6 and E7 proteins cooperate to immortalize human foreskin keratinocytes. EMBO J 1 Dezember, 1989;8(12):3905–10.
[49] Nyström A, Thriene K, Mittapalli V, Kern JS, Kiritsi D, Dengjel J, et al. Losartan ameliorates dystrophic epidermolysis bullosa and uncovers new disease mechanisms. EMBO Mol Med 20 Juli, 2015;7(9):1211–28.
[50] Nishie W, Kiritsi D, Nystrom A, Hofmann SC, Bruckner-Tuderman L. Dynamic interactions of epidermal collagen XVII with the extracellular matrix: laminin 332 as a major binding partner. Am J Pathol August, 2011;179(2):829–37.
[51] Gerum RC, Richter S, Fabry B, Zitterbart DP. ClickPoints: an expandable toolbox for scientific image annotation and analysis. Poisot T, Herausgeber Methods Ecol Evol Juni, 2017;vol. 8(6):750–6.
[52] Mittapalli VR, Madl J, Löffek S, Kiritsi D, Kern JS, Römer W, et al. Injury-driven stiffening of the dermis expedites skin carcinoma progression. Cancer Res 15 Februar, 2016;76(4):940–51.